

## Article

# Integrated Variable Speed Limits and User Information Strategy

Ernesto Cipriani, Lorenzo Giannantoni and Livia Mannini \* 

Department of Civil, Computer Science and Aeronautical Technologies Engineering, Roma Tre University, 00146 Rome, Italy; ernesto.cipriani@uniroma3.it (E.C.)

\* Correspondence: livia.mannini@uniroma3.it

**Abstract:** This paper deals with the study of variable speed limits (VSLs) for traffic control and their integration with user information strategies. As few studies have addressed the integrated VSL and user information strategy, we focus on comparing the adoption of the latter with the VSL alone strategy application and the no-control case, highlighting the benefits the integration brings. The integrated strategy is able to smooth the severity of congestion, shifting its occurrence in a section of the mainstream mostly suited to vehicle accumulation. An application on a real network is carried out. The traffic congestion conditions along the real highway are simulated by means of Dynameq simulation software and the METANET macroscopic model. The VSLs are applied in a control area aiming to evaluate the potential and the limitations of the strategy on a real network as well as the integration of variable speed limits and user information strategies. Two different cases of road congestion caused by the presence of on-ramps are studied. Results show that the integration of the two strategies leads to a redistribution of flows, achieving a reduction in the total travel time spent in the network and an increase in the traveled distances, i.e., reducing the overall network time despite the increase in assigned flows. However, an integrated strategy requires adequate transportation supply and mainly crossing demand.

**Keywords:** variable speed limits; user information; integrated strategies



**Citation:** Cipriani, E.; Giannantoni, L.; Mannini, L. Integrated Variable Speed Limits and User Information Strategy. *Sustainability* **2023**, *15*, 10954. <https://doi.org/10.3390/su151410954>

Academic Editors: Giulio Erberto Cantarella and Orlando Giannattasio

Received: 15 May 2023  
Revised: 5 July 2023  
Accepted: 10 July 2023  
Published: 12 July 2023



**Copyright:** © 2023 by the authors. Licensee MDPI, Basel, Switzerland. This article is an open access article distributed under the terms and conditions of the Creative Commons Attribution (CC BY) license (<https://creativecommons.org/licenses/by/4.0/>).

## 1. Introduction

In recent decades, the rapid increase in transportation demand has made the problem of traffic congestion increasingly relevant. Especially on highways, which were created to provide vehicular flow at high speeds, the occurrence of occasional or recurring congestion causes serious safety problems, increased levels of air pollution, and delays in travel times. A number of innovative control strategies have been developed to address these issues, encouraged by technological advances and the emergence of Intelligent Transportation Systems (ITS). Among these strategies are variable speed limits (VSLs), that is, the adoption of speed limits that can be changed over time by adapting them to weather and traffic conditions. The benefits brought by VSLs in the form of homogenization of vehicular flow have been widely demonstrated in the scientific literature. On the other hand, a possible alternative use of them relates to Mainstream Traffic Flow Control (MTFC), consisting of preventing the formation of bottlenecks in sensitive areas or mitigating their effects by slowing down the vehicular current upstream of them and thus creating potentially less congestion on controlled road sections.

The analysis of previous studies shows that there is a lack of an integrated traffic management system that combines VSLs with other Intelligent Transport Systems (ITS) in order to provide a complete active traffic and demand management system.

The paper deals with the study of VSLs within an MTFC strategy along a highway network, focusing on the integration with user information strategy. An application on a real network was carried out and two critical conditions were observed: the first close to the control area and the second distant from the control area, highlighting the positive and negative aspects of each conditions. Specifically, the case study concerned the Venetian

highway network surrounding the locality of Mestre (VE) and including the A4 Highway (Mestre Bypass), the A57 (Mestre Ring Road), and the A27 Highway in Italy. First, the traffic congestion conditions along the A57 were simulated by means of Dynameq simulation software and the METANET macroscopic model. Next, the variable speed limits were applied in a control area aiming to evaluate the potential and the limitations of the strategy on a real network as well as the integration between VSLs and user information strategies. The speed limits were modified to ensure that the desired speed in the critical section was gradually achieved in the space and time as drivers must be accompanied progressively to the desired speed limit in the section of interest. Therefore, speed changes must be gradual in space (between successive sections) and time (in the same section) in order to ensure the flow smoothness and safety of the vehicular stream and to promote the acceptance of speed limits by users.

The reminder of this paper is structured as follows. Section 2 reports the literature review related to the VSL topic. Section 3 presents the methodology applied, while Section 4 describes the case study analysis. Finally, Section 5 summarizes the conclusions and further developments.

## 2. State of Art

Variable speed limits are an ITS solution that allows the dynamic variation of imposed speed limits in response to adverse weather conditions, accidents, or increased traffic. To determine the most appropriate speed for vehicle transit, VSL systems use speed, volume, and weather detectors along the infrastructure. In addition to these detectors, the adoption of variable speed limits requires variable message signs on which to display the imposed limit. The main benefits of VSLs can be summarized as improving safety, addressing traffic breakdown problems [1], decreasing the environmental impact [2], and increasing flows. For example, Kotsialos et al. [3] identified a direct relationship between total network time and inflow and outflow values of the reference section, highlighting the achievable benefits.

VSL control strategies belong in two basic categories: reactive or proactive approaches.

Historically, the first approaches followed a reactive logic. Based on measured values of flow, occupancy, or speed, these strategies established values of pre-determined speed limits with the aim of improving traffic safety. The first applications were recorded in the Netherlands thanks to the impact of the action plan proposed by the Dutch Ministry of Transport in 1982 aimed at reducing the effect of congestion levels on the infrastructure. Smulders [4] conducted one of the first experiments in automatically varying speed limits on several stretches between Utrecht and Amsterdam. In [5] the authors developed a strategy whose goal was not to reduce average speed but to minimize the speed difference between vehicles in the same or adjacent lanes. Bertini et al. [6] evaluated the effects of variable speed limits placed along Autobahn 9 for eighteen kilometers in the neighborhood of Munich. In [7] the authors proposed a VSL strategy with default values to attempt to solve congestion problems in the area adjacent to the Orlando metropolitan area in America.

The rule followed is to impose a speed limit close to the eighty-fifth percentile of measured speeds. A fundamental problem related to the adoption of VSLs with predefined rules was found by Dong et al. [8] in a study conducted within the city of Beijing. Indeed, from the study it was found that users tended to disregard the imposed speed limits when the driver did not perceive a danger such that he or she had to reduce his or her speed and when the VSL system was adopted continuously over days, which generated a habit of ignoring the presence of such a signal. This second condition is particularly alarming because it highlights the effectiveness of the strategy only when used for limited times and under conditions of special need, which also emerged in [9].

Proactive VSL strategies arise to determine speed limits with greater detail and optimize the instants of control activation according to the results provided by demand forecasting. Therefore, it is very important to predict the traffic flow conditions [10,11] and the demand [12,13]. In order to integrate this type of strategy with transportation demand forecasting, it is necessary to model traffic behavior, and this is done from the

basic diagrams representing steady-state conditions. An initial assumption of behavior at zones subjected to speed limits was proposed in [14] and then adapted to VSLs in [15]. The assumption is to scale the fundamental diagram as a function of the imposed speed limit. Instead, the study conducted in [1] led to the assumption that the desired speed is equal to the minimum value between the speed corresponding to the traffic conditions and the speed imposed by the limit, i.e., that the disposed flows are reduced only in the case of a detected speed greater than that imposed by the limit.

In [16] the authors showed the impact of VSLs on aggregate traffic behavior based on field observations on a highway in terms of achieving higher densities at the maximum capacity drop, as well as an increase in the latter in some sections. This increase, however, was only apparent and due to the prevention of capacity drop phenomena.

Such a formulation was used in [17] along with an EKF to test the adaptive capabilities of the model to a highway corridor, offering a considerable correspondence of simulated values with measured values.

In [18] the adoption of a Cell Transmission Model (CTM) was presented, in which the conservation equations considered the maximum flow value as a function of speed limit.

Bie et al. [19] developed a variation of the METANET model by integrating it with the Stochastic Cell Transmission Model (SCTM) for traffic prediction. A different objective function was determined in [20], whose formulation linked accident risk with the adoption of VSLs. The study by the authors of [21] showed a potential reduction in total network times of 25% in urban areas. In [22] the authors evaluated two different VSL strategies for resolving multiple bottlenecks along the same corridor based on flow or density values. Carlson et al. [23] proposed a new control measure called Mainstream Traffic Flow Control (MTFC).

The development of VSLs has mainly involved macroscopic models; however, this control strategy is also reflected at the microscopic level. In this regard, in [2] the authors integrated the METANET model with the microsimulation model “Virginia Tech” (VT-micro), which can determine the amounts of pollutant emissions when variable speed limits are adopted on the road transport infrastructure. Moreover, with the improvement of new technologies, the development of Autonomous Vehicles (AVs) and Connected Vehicles (CVs) perspectives for traffic control are emerging. The presence of such vehicles has effects on both macroscopic and microscopic variables and models. Lu et al. (2018) [24] studied the effects on the fundamental diagram of AVs. Olia et al. [25] analyzed their impacts on capacity. In [26] the authors analyzed mixed traffic flows, applying a microsimulation approach to estimate traffic flow parameters. In [27] a review of VSL and RM control models is presented; in addition, the authors summarized the best practices for mixed traffic flow control and provided new insights and future research perspectives.

The possible development of VSLs in the CV environment makes acquiring information about the location and speed of vehicles very important. In a recent study [28], the authors presented a platform to achieve and process automated driving system data in order to reconstruct the trajectories of CAVs. Ref. [29] proposed a vehicle localization system considering vehicle lateral velocity.

In [30] the authors studied a VSL control applying a microscopic approach, specifically by means of the Model Predictive Control (MPC) approach in the Connected Vehicle (CV) environment. In [31] the authors presented VSL strategies by adapting the FD of the cell transmission models (CTMs). The authors adopted the MPC approach and the strategies applied were combined with many significant phenomena, including shock wave formation and capacity drop.

However, few studies have addressed the integration of VSLs with user information. We can mention the following. In [32] the authors proposed adopting the VSL strategy along with the lane change strategy, highlighting the benefits that can be achieved by providing information to users spatially in advance. Raadsen et al. [33] proposed the adoption of a Link Transmission Model (LTM) in which the search for greater realism comes from the propagation of speed limit knowledge among users rather than instantaneously transmitted information. In [34] the authors presented an overview of VSLs; among several

recommendations for future research, the authors pointed out the lack of an integrated traffic management system that combines VSLs with other ITS devices, such as ramp metering, lane control, on-board information devices, and dynamic route guidance.

Thus, we focused on studying the adoption of the VSL strategy integrated with user information, highlighting the benefits the latter brings.

The proposed strategy is not able to prevent the occurrence of congestion but aims to contain it by generating it in a section of the mainstream where vehicles can accumulate. In contrast to ramp metering, the mainstream is in fact capable of accumulating more vehicles in the queue.

### 3. Methodology

The use of VSLs to control traffic flow conditions requires the definition of three basic elements:

1. Network loading or traffic simulation model, necessary in order to predict the progression of vehicles along the infrastructure, to determine aggregate variables (flow, density, and speed), and to study the reaction to the adopted control strategy.
2. Control strategy, which must define the criteria under which VSLs operate and the conditions for VSL activation.
3. Traffic behavior model, in order to define how VSLs affect user behavior.

As for the simulation model, the second-order macroscopic model METANET [35] was mainly dealt with in the study. A macroscopic first-order Lighthill, Whitham, and Richards (LWR) model and the microscopic models used by the simulation software Dynameq (lane change model, interval acceptance model, and queued vehicle model) were also observed to try to improve its application. Specifically, a minimum speed value was set for the METANET model, the flow in the origin links was constrained by the density on the infrastructure, and, finally, a queuing model was included. The first-order model used was an implementation of the LWR solver via the Lax–Hopf method [36].

Figure 1 shows the logical architecture of the methodology. First, the demand is loaded onto the supply by means of the dynamic assignment model providing the distribution among the different paths. Next, METANET model application provides the traffic state progression. Then, the density is monitored in order to identify the critical sections. After, the strategy determines the suggested value of speed. Finally, the speed limit is calculated according to the distance between the critical section and the VMS. It is necessary to verify some constraints, as described in detail in Section 3.2, once the strategy has been applied; the traffic behavior model defines the VSL effect to user behavior.

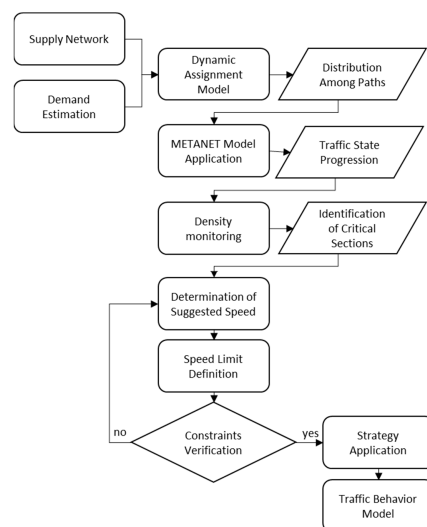


Figure 1. Logical architecture.

### 3.1. Adopted Model

Dynameq software (version 4.3.1, Bentley Systems, Exton, PA, USA) was used to assign the demand and determine the distribution among the different paths, while the METANET model was used to simulate vehicle advancement. Therefore, the equations adopted are:

State equation:  $q_i(t) = v_i(t)k_i(t)\lambda_i + \zeta_i^q(t)$

Continuity equation:  $k_i(t+1) = k_i(t) + \frac{\Delta t}{L_i\lambda_i}(q_{i-1}(t) - q_i(t) + r_i(t) - s_i(t))$

Payne's equation for the estimation of dynamic speed:

$$v_i(t+1) = v_i(t) + \frac{\Delta t}{\tau} \{v_e[k_i(t)] - v_i(t)\} + \frac{\Delta t}{L_i} v_i(t) [v_{i-1}(t) - v_i(t)] - \frac{\eta \Delta t}{\tau L_i} \frac{[(k_{i+1}(t) - k_i(t))]}{k_i(t) + \kappa} - \frac{\delta \Delta t}{\lambda_i L_i} \frac{r_i(t) v_i(t)}{k_i(t) + \kappa} + \zeta_i^v(t) \quad (1)$$

where

$q_i, v_i, k_i$  are respectively the flow, the speed, and the density of  $i$ th segment;

$r_i, s_i$  are respectively the flow of the on-ramp and of the off-ramp of  $i$ th segment;

$L_i$  is the length of  $i$ th segment;

$\lambda_i$  is the number of lanes of  $i$ th segment;

$\kappa, \tau, \eta$  are the model parameters;

$\zeta$  is the model noise, with a normal distribution characterized by a zero mean and  $Q$  covariance.  $\zeta(t) \approx N(0, Q(t))$ .

The desired speed is determined as:  $v_e(k) = v_f(t) \exp\left[-\frac{1}{\alpha} \left(\frac{k}{k_{cr}}\right)^\alpha\right]$ .

These equations are subject, for each time instant  $t$ , to the constraint  $v_i(t) > v_{min}$ , with  $v_{min} = 1$  km/h.

Moreover, the boundary conditions impose that in segment 1 the convective term is absent ( $v_0(t) = v_1(t)$ ) and that in the last segment there is no kinematic wave of congestion from downstream, thus the absence of the anticipation term ( $k_{end+1}(t) = k_{end}(t)$ ).

The main problem encountered using the METANET model is the magnitude of flow coming from the on-ramp and not constrained by the characteristics of the mainstream. In [3] the authors proposed to split the network into highway links and origin links. The former is characterized by the equations of the METANET model. On the other hand, the origin links receive the demand and forward it into the network, and they are characterized by their capacity and queue length. A queuing model is applied for these links and the outflow is determined as:

$$q_o(t) = \min\left[q_{od}(t) + \frac{w_o(t)}{T}, q_{max,od}(t)\right]$$

where

$q_{od}(t)$  is the demand in time interval ( $t$ ),

$w_o(t)$  is the queue length (in vehicles),

$q_{max,od}(t)$  is computed as:

$q_{max,od}(t) = C$  if  $k_\mu(t) < k_{cr}$ ,

$q_{max,od}(t) = C \times p(t)$  otherwise,

With  $C$  as the capacity of origin link and  $p(t)$  as the portion of flow that can enter the  $\mu$  link immediately downstream of origin, i.e.,  $p(t) = \frac{k_{max} - k_\mu(t)}{k_{max} - k_{cr,\mu}(t)}$ .

The conservation equation for the origin link is also added to express the formation of the eventual queue:

$$w_o(t+1) = w_o(t) + T \times [q_{od}(t) - q_o(t)]$$

The above equations modify the flow constraint for the mainstream and provide an updated flow of the on-ramp.

An initial analysis was performed on a test network to calibrate a robust simulation model that is generalizable to real networks as well. Transportation demand was varied, thus allowing the behavior of the model to be evaluated under different traffic conditions.

The test infrastructure was a stretch of highway with a total length of 3 km and consisting of two travel lanes for the entire development. It was divided into 6 segments of equal length of 500 m. An on-ramp was placed at the beginning of the fifth segment while an off-ramp was placed at the beginning of the second segment.

Three test scenarios were analyzed. Specifically, the first scenario was carried out trying to achieve capacity operation of the infrastructure. The second simulated scenario aimed to simulate a critical situation on the infrastructure by also modifying the on-ramp flows. The last scenario was carried out with the aim of verifying the recurrence of this phenomenon. The demand in the third scenario was increased by making the flow on the ramp comparable to that of the mainstream.

As can be seen from Figure 2a, the simulated points follow the trend of the function with respect to the steady states of the fundamental diagram of segment 5. This can also be seen in the speed-flow diagram of the same segment shown Figure 2b, where a well-defined trend emerges for the lowest speed values.

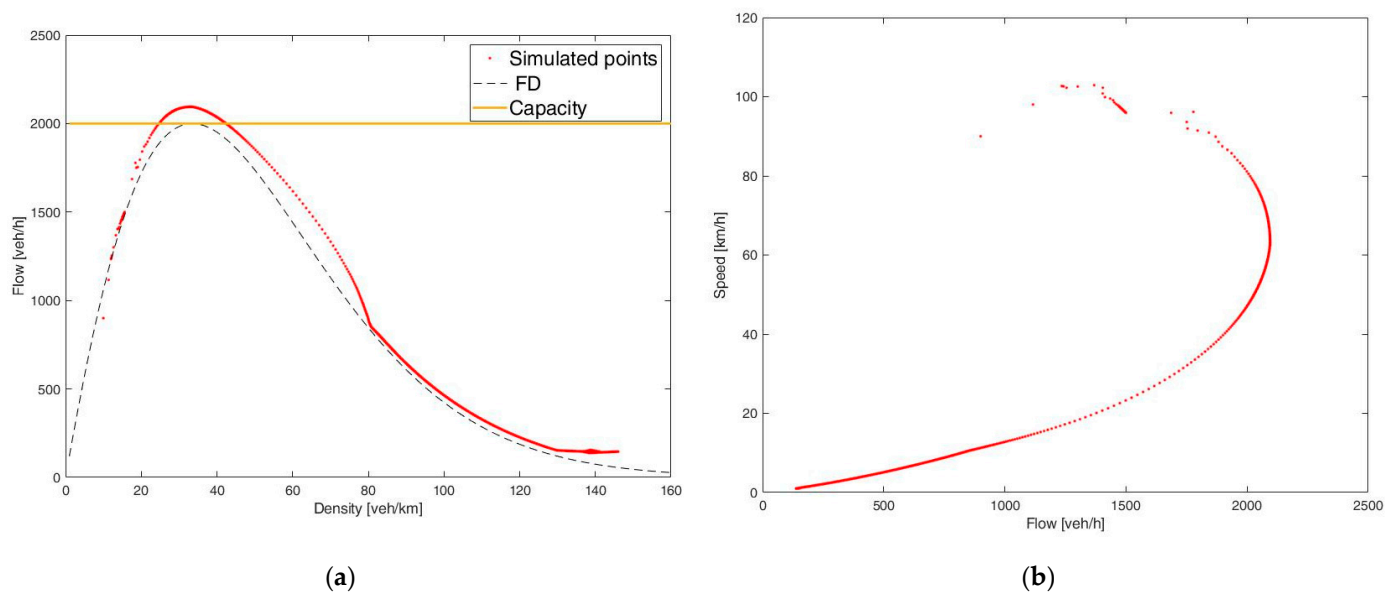


**Figure 2.** (a) Flow-density diagram of segment 5; (b) Speed-flow diagram of segment 5.

### 3.2. Control Strategy

Once the demand values and initial density and speed conditions on the network have been defined, the progress of vehicles over time is simulated by monitoring the change in density values within the network segment where the strategy has to be activated. First the critical sections are identified when in a monitored segment the density is  $k_i > \rho k_{cr}$ , where  $\rho$  is a threshold coefficient ranging from 0 to 1. Next, the capacity of the critical sections identified is determined as  $C_s(t) = k_i(t) \times v_i(t)$ . Then, the minimum value between that calculated and 90% of the maximum capacity of the section is selected ( $C_i(t) = \min\{C_s(t), 0.9 \times Q_{max}\}$ ). After, the strategy determines the suggested value of speed. Specifically, the number of vehicles ( $N_{cr}$ ) between the critical section and the nearest variable message sign (VMS) going upstream is computed as the sum of the products between the density of each segment and its length ( $N_{cr}(t) = \sum k_i(t) \times L_i$ ). The time required to dispose of these vehicles is calculated as the ratio between this number of vehicles and the previous calculated capacity ( $t_d = N_{cr}(t)/C_i(t)$ ). Thus, the speed limit is calculated as the ratio between the distance ( $d_{cr} = \sum L_i$ ) between the critical section and the nearest VMS and  $t_d$  ( $V_{VMS} = d_{cr}/t_d$ ). Finally, it is necessary to verify that some constraints are met. First among them is that the speed value ranges from a lower limit that can be imposed on the speed to avoid excessive decay of the infrastructure performance to a maximum value established by the administrative limit. Second, for each sign, the speed limit is compared with the one previously reported, verifying that the difference in their speed is not greater than a threshold ( $\Delta V_t$ ). Moreover,

a comparison is also performed between adjacent VMS, imposing the maximum difference between the two speeds equal to a threshold difference ( $\Delta V_s$ ). The reason for the inclusion of the latter constraints is twofold:

- to encourage the acceptance of speed limits by users, who might otherwise find its rapid reduction unjustified;
- to maintain a high safety standard, since a rapid transition between two different speeds could increase the risk of accidents because of different user behavior, thus spatially anticipating the risks that would otherwise occur at bottlenecks.

The control phase is repeated following a minimum interval of five minutes from the previous update, which is necessary so that the two conditions above described are ensured.

### 3.3. Traffic Behavior Model

Among the models proposed in the literature, the most interesting for describing the behavior of traffic subject to VSLs is the model of [1], based on the empirical assumption that the speed limit affects only those users who travel at a speed greater than the imposed limit, and the model proposed in [23], built from direct field observations. These two models were subjected to testing to determine the best fit for the purposes of the study. By comparing the results obtained with the two different behavior models, it was noted that they were able to return entirely similar results. The chosen model was the Carlson's model, which assumes that as speed limits vary, the fundamental diagram (representing the desired speed to which the user tends) also changes. This variation, assumed from the data collected on traffic behavior, does not occur by linearly scaling the curve of the fundamental diagram but rather by shifting the critical density toward larger values.

If under normal conditions the desired speed can be determined by the relation reported above  $v_e(k)$ , denoting by  $b$  the ratio of the imposed speed limit to the speed of the free current, the relation becomes:

$$v_e(k) = v'_f(t) \exp \left[ -\frac{1}{\alpha'} \left( \frac{k}{k'_{cr}} \right)^{\alpha'} \right] \quad (2)$$

with  $v'_f = v_f \times b$ ,  $k'_{cr} = k_{cr} \times [1 + A \times (1 - b)]$  and  $\alpha' = \alpha \times [E - (E - 1) \times b]$ , where the parameter  $A$  determines the magnitude of the deviation of the critical density, usually ranging from 0.6 to 0.7 and in this study set equal to 0.67, as in [23], while the parameter  $E$  determines the disposal capacity and it is set equal to 1.5. Figure 3 shows that as the travel limit speed decreases, the critical density progressively increases from 33.5 veh/km (obtained with the speed  $v_f = 110$  km/h) to a maximum value of 57 veh/km with  $v_f = 10$  km/h. This effect is due probably to the more cautious users' behavior in the case of a lower speed limit.

The objective of the following test phase was to delineate the behavior of users as speed limits varied, thus contemplating deviations from realistic speed limit values. For the same reason, the maximum speed differences were set equal to 30 km/h, tolerating a large difference between adjacent variable message signs and between limits imposed at two consecutive time instants. The section subjected to the control strategy was between section 2 and section 10. To realize the bottleneck, an initial operation at capacity of the infrastructure was assumed, with a sudden increase in flow coming from the ramp of section 15 after reaching an initial stationarity. We focused on the results obtained in flow-density diagrams from sections 7 to 12, i.e., of the sections including the last segments under control and the two immediately downstream.

Figure 4 shows the flow-density trend compared to the fundamental diagram obtained under steady-state conditions (dotted line): the condition with no control is shown in red while the controlled one is in blue. It can be seen that there was a lower capacity in the controlled conditions because of the lower speed at which vehicles could travel. In the transition from one speed limit to the next, simulated points are also visible that exhibit the same density albeit with a reduction in capacity. They represent the transition from one fundamental diagram to the next. In the controlled condition, nearly the same outflow

(throughput) of the no-controlled one was approached but remained in the steady branch of the diagram, thus avoiding possible flow instabilities. Then, the vehicles thickened (the density increased but still remained below the critical value) moving along the stable branch of the curve.

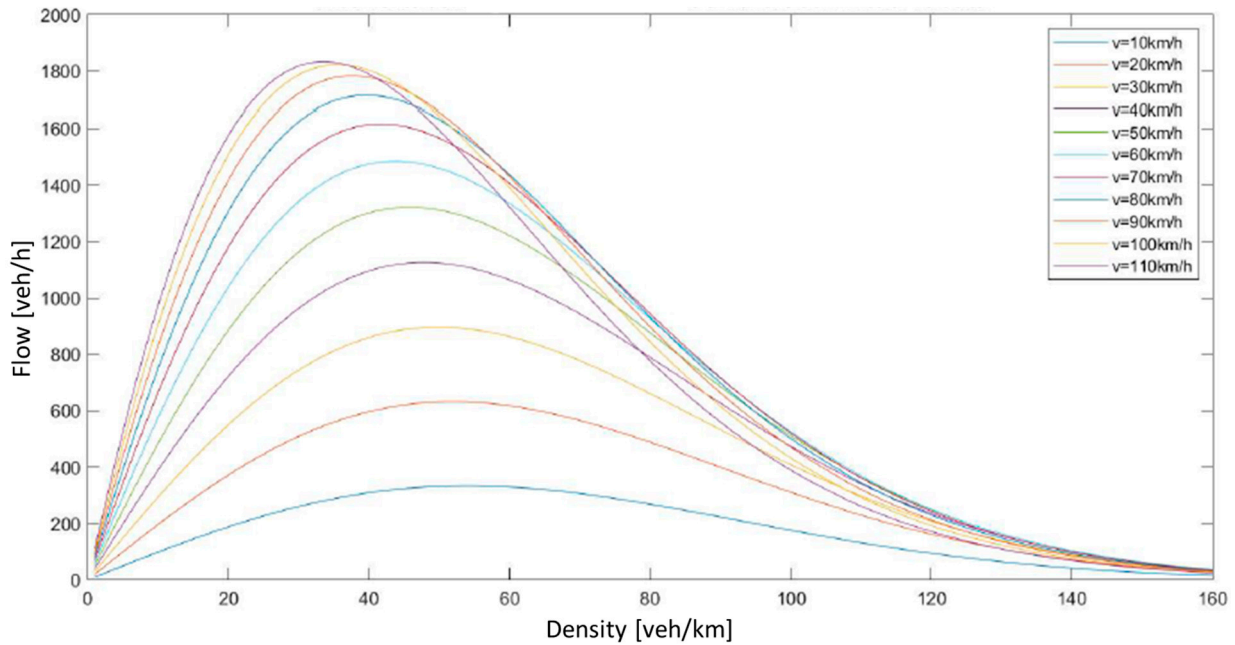


Figure 3. Variation of the fundamental diagram according to Carlson's model application.

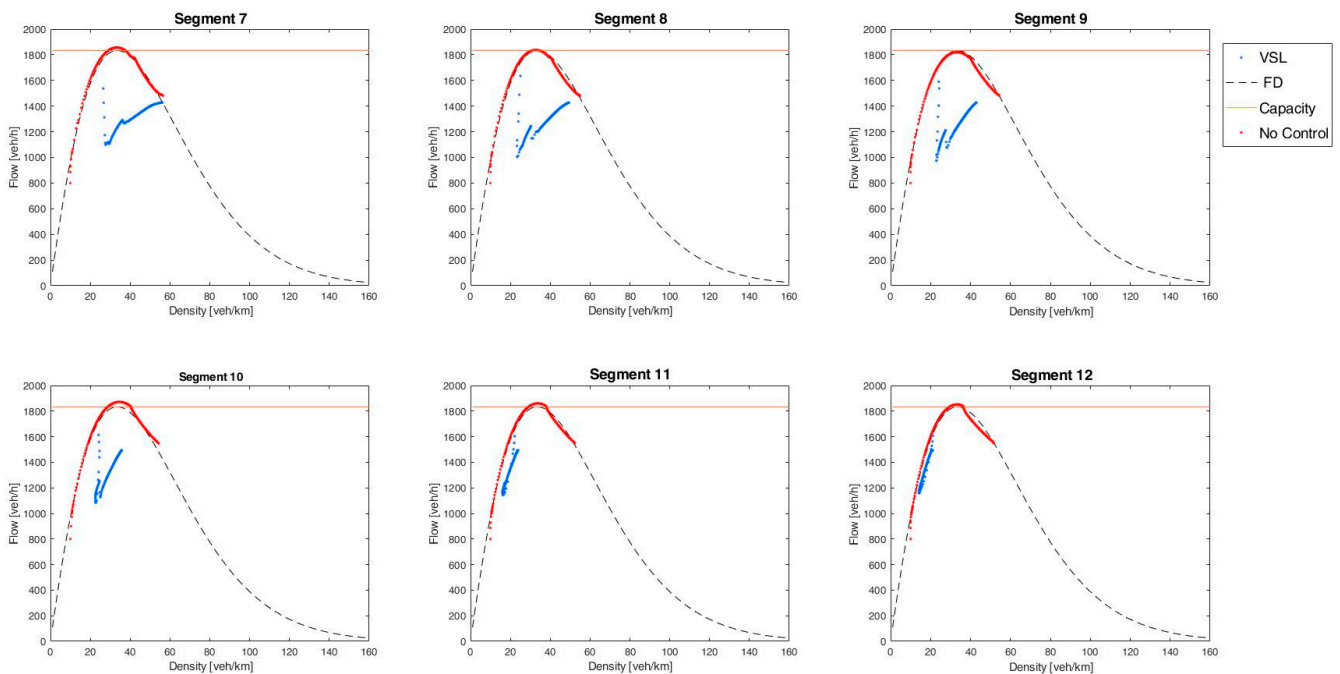


Figure 4. Fundamental diagrams from section 7 to section 12.

#### 4. Case Study

The case study concerned the A57 Highway, which acts as an interconnection between the city of Venice and the A4 (east and west) and A27 (north) highways (Figure 5).



**Figure 5.** Framework of the A57 Highway and Dynameq's graph.

This infrastructure was monitored by a control system called M.A.R.C.O. by means of sensors located along the infrastructure. The detected data combined with the images provided by the traffic surveillance cameras allowed the adoption of control strategies such as VSLs, ramp metering, or dynamic lane.

The road network included the A4 Highway from kilometer 363 + 800 m to kilometer 418 + 300 m, along with the A57 Highway from kilometer zero to kilometer 26 + 700 m and the numerous interchanges along these highway sections. Between kilometer 6 and kilometer 18 of A57, there were 12 VMS, about every 1500 meters. Based on the classification of links proposed by [3], the network was divided into highway, origin, and destination links.

The area was divided into 24 zones and the demand was reconstructed. For each study scenario, the demand was assigned on Dynameq, recording the splitting rates at the nodes and the simulated outflows on the accumulation links, thus simulating the demand prediction phase. These values fed the METANET model on MATLAB.

The study evaluated the effects of VSLs on two main cases. In both, stationary conditions with disposal values close to capacity were simulated. Under these conditions the demand value of one of the ramps was increased, causing spillback congestion. These conditions persisted upon the occurrence of a kinematic wave because of a high reduction in upstream and on-ramp demand. The simulation occurred over a 12 h time horizon, overstating the demand levels in order to study the potential of the control strategy.

In the first case analyzed, a bottleneck was assumed to form at kilometer 16 + 500 m at the intersection with the SS13, a road connecting the city of Venice with the municipality of Udine and the Austrian border. The importance of preventing the formation of a queue at this intersection was related not only to the difficulties of entering from the ramps but also to the obstacle generated for vehicles that needed to exit the highway using the off-ramps.

The second case concerned the intersection with the A27 at kilometer 20 + 300 m. Similar to the first case, this is a major intersection and its structure is such that it presents an off-ramp immediately upstream of the on-ramp. As upstream no additional ramps are present for nearly 6 km, this intersection was suitable for a mainstream traffic control strategy.

For the application of the control strategy, the VMS used are reported in Figure 6 in order to evaluate the effectiveness of the control strategy in two main cases, namely, with bottleneck formation immediately downstream of the control area or several kilometers after it, thereby assessing the potential of VSLs as a response to the possibility of congestion at a distance from the point of intervention.

The results returned by the simulation scenarios were evaluated by observing the performance on the two main corridors through two indicators: Total Time Spent (TTS) and Total Travel Distance (TTD). The ideal intervention condition occurred when a decrease in TTS coincided with an increase in TTD, a situation that expresses a reduction in travel time despite an increase in vehicles on the network.



**Figure 6.** Location of intersections and variable message signs used for the strategy.

#### 4.1. Results in Case of No-Control Strategies

The scenario with no-control strategies application was not calibrated; we applied the parameters reported in the literature [37]. Figure 7 shows the density trend in space and time along the A57 corridor. As can be seen, in the first hour of the simulation and thus until an equilibrium state was reached, the area adjacent to the Mestre location (between segments 44 and 59) was characterized by flows close to capacity, identifiable by the near-critical density values. As a result of the increase in demand at the intersection (segment 55), a kinematic wave was generated that, with different speeds depending on the variation in demand values, propagated upstream. At simulation interval 2500, the halving of demand on the main current was simulated. This phenomenon originated a congestion dissipation wave that started from the first section and, when it met the congestion wave near section 38, reduced its propagation speed by improving the performance of the vehicular current until the initial conditions were restored. The diagram thus shows how the congestion state propagated uncontrolled upstream for nine kilometers, remaining at the intersection until the arrival of the dissipation wave from upstream.

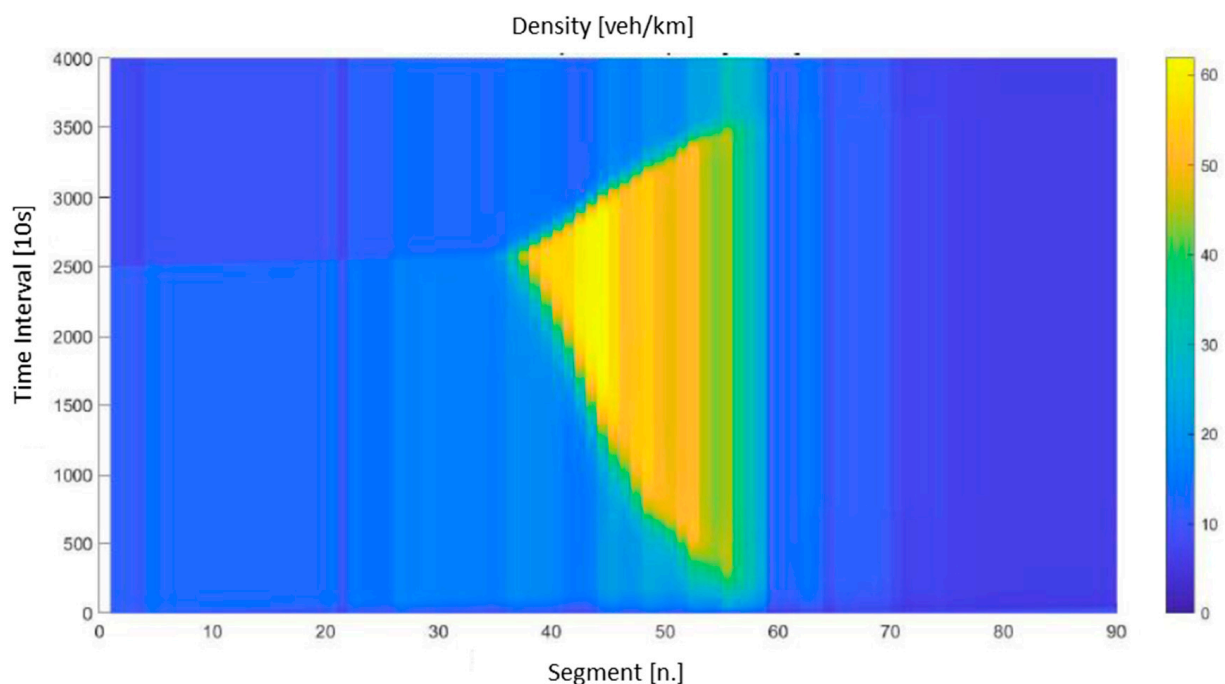


**Figure 7.** Density trends in time and space of the A57 in the case of no-control strategies.

It was observed that although the congestion originated in section 55, the density was increasing upstream, showing how the kinematic wave was not constant but was amplified by interacting with additional oncoming vehicles.

Two areas with significantly lower densities also emerged along the corridor: the first 20 segments and the last 20, which were part of the A4 Highway and had a higher speed limit and capacity. The graphical division into sections with distinct density values, on the other hand, was a limitation of the METANET model, which unlike the Cell Transmission Model did not predict an exact continuity in the values of two adjacent segments but rather a “stepped” variation.

Figure 8 shows, from section 46 to section 51, the trend of traffic states, evaluating the simulated flow values as a function of the corresponding densities. The simulated states are shown in red while the fundamental diagram of the sections is shown with the dotted line. The capacity of the infrastructure is shown in orange, highlighting how in each segment it is much higher than the maximum flow. This is the capacity drop phenomenon whereby the infrastructure failed to utilize the entire remaining capacity in the transition from stable to congested conditions.

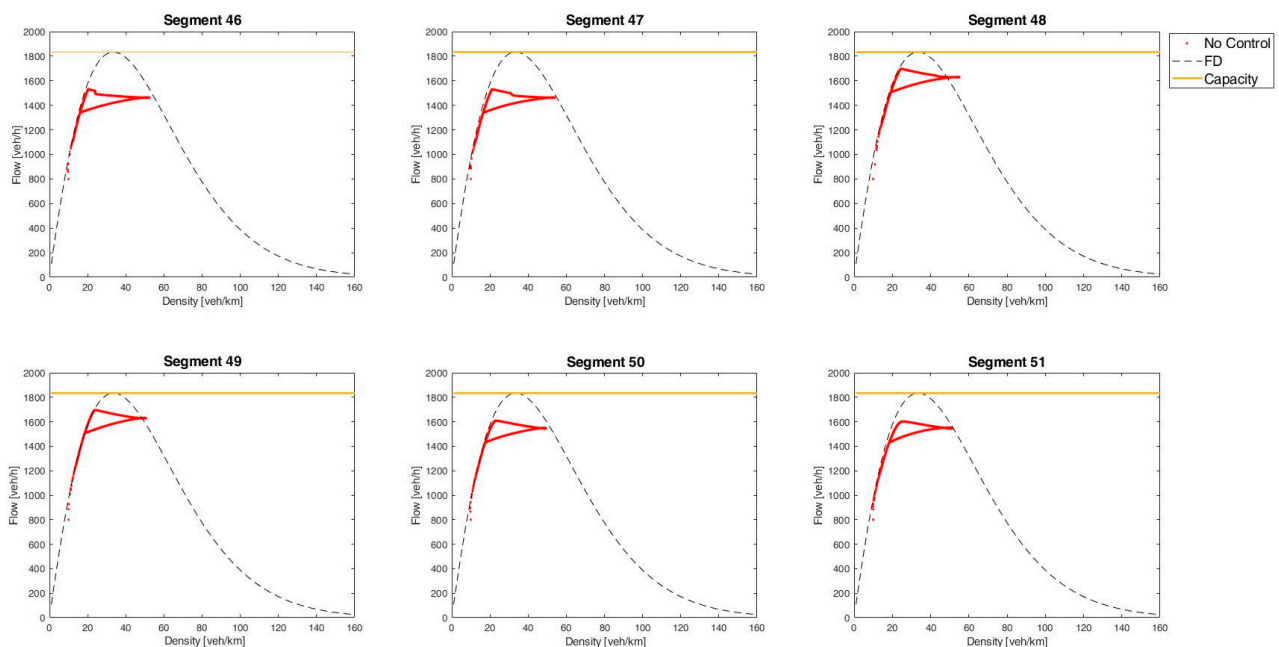


**Figure 8.** Fundamental diagrams from segment 46 to segment 51. Capacity drop phenomenon.

#### 4.2. Results in Case of VSL Strategies

The first control strategy adopted involved the use of VSLs. Comparing the density values in Figure 9 with those in Figure 7, it can be seen that in the Ring Road, the congestion state propagated more upstream but reduced density immediately downstream of the control sections. Similar to the behavior verified in the absence of control, the propagation of this state occurred until the disposal wave was reached, which was generated by the reduction in demand values. This condition occurred up to section 30, causing persistent high-density values over time. Thus, induced congestion occurred upstream of the control area, but a sharp reduction in density values can be seen in the sections after 49.

The only segment downstream of the control area in which no benefit was obtained was the 55th, i.e., the section with the intersection that caused the bottleneck. Therefore, the traffic behavior in that section was investigated in depth. Specifically, the evolution over time of density, queuing on the on-ramp, and flow were evaluated.

Important considerations emerged from the comparison of each variable: the density decreased slightly following the activation of current control, probably because of the magnitude of flows that were allowed to reach the section. This state persisted longer

as hypothesized, and thus, a longer time was required before a steady-state condition with lower density values was restored. However, there was no direct evidence of this by observing the flow disposed of by the section, which remained almost identical to natural conditions up to the 3500 intervals. After that interval, higher values of flow disposed were simulated, corresponding to the delay in restoring the steady-state conditions.

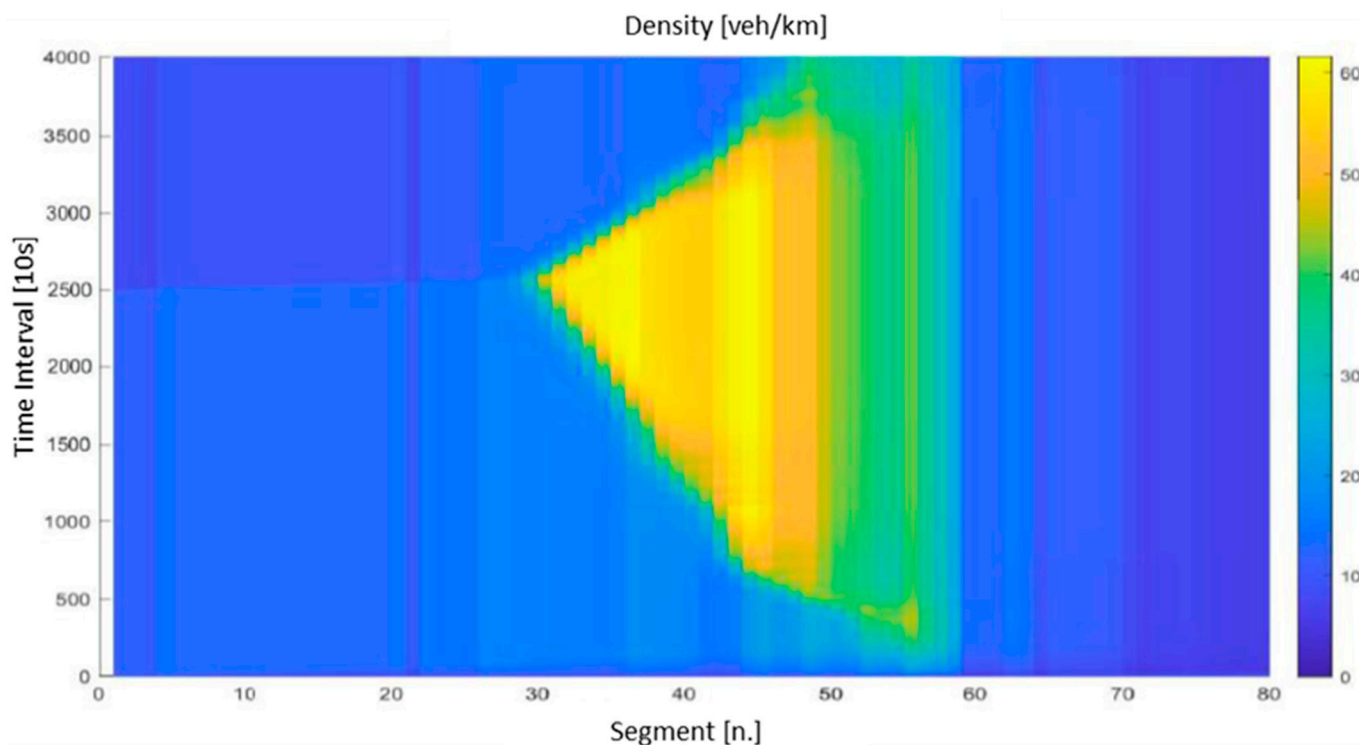


**Figure 9.** Density trends in time and space of the A57 in the case of VSL strategies.

The reason why a controlled flow came from upstream but the same amount was disposed of in the section was then evident only by considering the queuing trend in the ramp entering the section. In fact, the increase in queue length over time was very slow when compared to the simulation in the absence of control and reached a maximum length of sixty-two vehicles, i.e., a 75% reduction from the critical extension reached. It was also fully reabsorbed within the simulation period, and the attainment of steady-state conditions occurred upon its complete disposal. Thus, the reason why there was no net reduction in density was precisely because of the greater number of vehicles from the ramp that managed to enter, keeping the comparative flow values unchanged.

The benefits of adopting VSLs were fully achieved at the intersection, but the effects also needed to be evaluated within and upstream of the control sections. With particular reference to the last three kilometers subject to the strategy (from section 46 to 51), traffic evolution was observed with flow-density diagrams (Figure 10, where the simulated states are shown in blue in the dotted line in the fundamental diagram in the absence of speed limits).

Comparing the simulated traffic states with the trend of the FD obtained by maintaining  $V_{free} = 110$  km/h, they appeared to correspond to transient points located within the FD. Actually, the model proposed by Papageorgiou assumed a change in the curve with an increase in the critical density value. Thus, the states represented as a result of the reduction in the speed limit were not unstable but rather representative of the stable conditions obtained despite a higher value of density. In such a situation, in fact, the maximum value of the section's disposal capacity was reduced, nevertheless improving the interaction between vehicles and promoting safer progress at the same maintained spatial spacing.

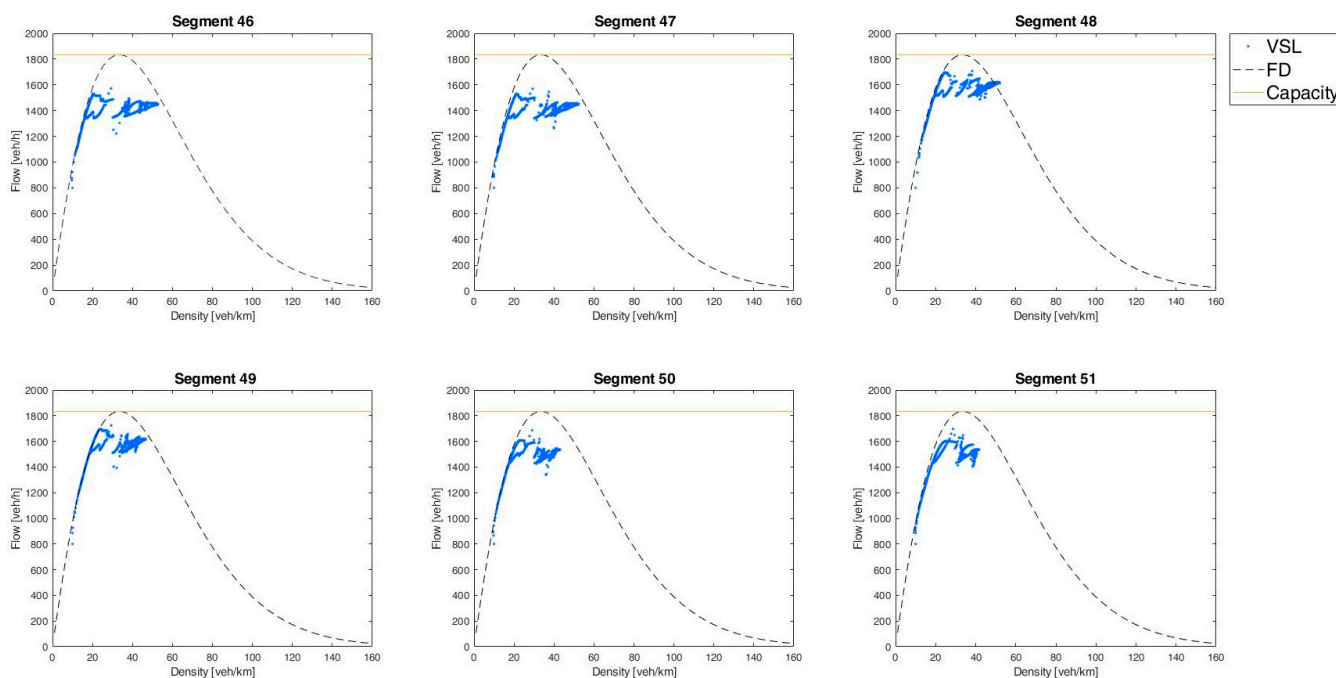


**Figure 10.** Fundamental diagrams from segment 46 to segment 51.

Indeed, activation of the control strategy was followed by an initial lowering of the disposal flows followed by the attainment of a steady state, which persisted until the arrival of the kinematic wave of congestion disposal. Corresponding to this steady state, the flows remained at the same values as they were without the control strategies, however, persisting longer than with the latter.

Regarding the effects of the variable speed limits on the Mestre Bypass, they were exhausted before reaching the interchange and therefore did not vary the performance of this corridor, thus being unaffected.

A final assessment of the benefits of the possible intervention concerned the performance of the network as a whole and thus in terms of TTS and TTD. As can be seen from the summary Table 1, the adoption of VSLs caused in this circumstance an increase of 1.38% in Total Time Spent, while the total distance traveled was almost unchanged (only 0.02% more). However, VSLs increased network time but significantly reduced the time spent by vehicles queuing on ramps, which could be perceived more severely by users.

**Table 1.** Comparison of TTS and TTD indicators on major corridors and at the network level between No Control and VSL strategies application.

	No Control	VSL	Variation [%]
TTS on Ring Road (A57) [veh × h]	33,530	34,740	3.61%
TTS on Bypass (A4) [veh × h]	53,850	53,850	-
TTS on Network [veh × h]	87,380	88,590	1.38%
TTD on Ring Road (A57) [veh × km]	2,470,130	2,470,820	0.03%
TTD on Bypass (A4) [veh × km]	768,040	768,040	-
TTD on Network [veh × km]	3,238,170	3,238,870	0.02%

#### 4.3. Integrated VSL Strategy and User Information

The second intervention proposal attempted to evaluate the integrated effects of VSLs with user information on the presence of congestion, thus trying to take advantage of the residual network capacity offered by the A4 Highway. To this end, the control strategy was implemented on Dynameq software in order to simulate the same demand matrix but with the activation of VSLs. Therefore, the conditions used on METANET were reproduced to determine the different distributions of demand on the routes. In this way, it was assumed

that the user could be provided with information on the level of congestion on the network before reaching the junction between the A57 and the A4 by changing the splitting rate values adopted in the macroscopic model. The user variation was significant, motivated by a high crossing demand that preferred to travel the greater distance offered by the A4 Highway as long as the times were shorter. The assumption made was to start providing information to the users after three hours from the start of the simulation, and the results showed clear differences from what had already been observed: in fact, from Figure 11 it can be seen that in the first three hours of the simulation the density trend was identical to that shown in Figure 9.

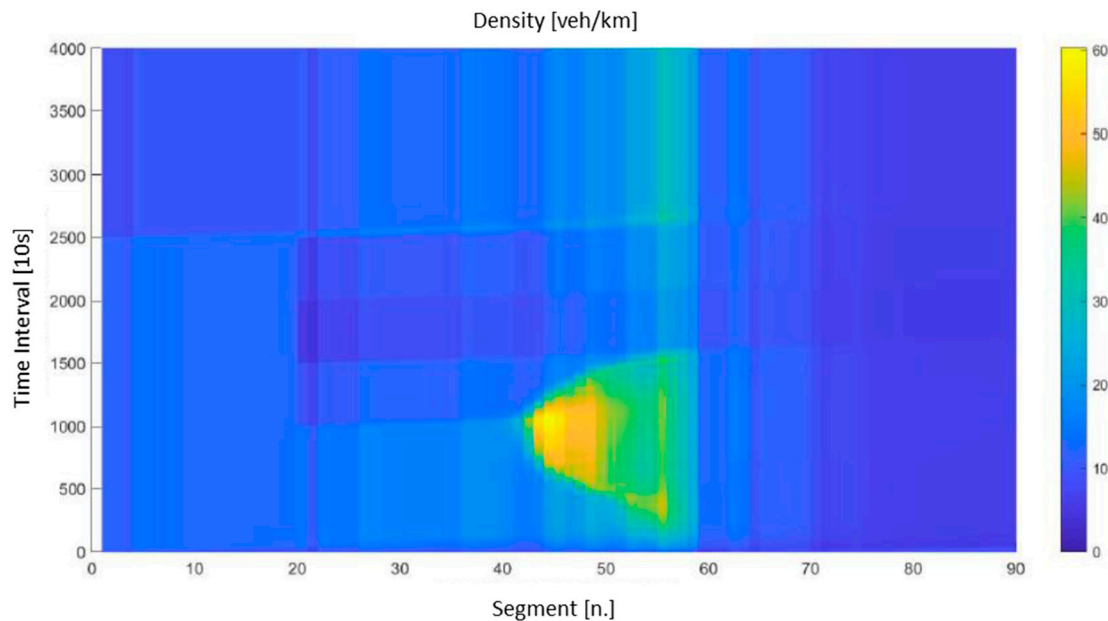


**Figure 11.** Density trends in time and space of the A57 in case of Integrated VSL strategies and user information.

The change in splitting rate generated a kinematic wave that propagated quickly downstream from section 19, i.e., the junction between the Ring Road (A57) and the Bypass (A4). It quickly reached the congested area and managed to resolve the situation before the arrival of the next kinematic wave, which further reduced the density values. The restoration of the initial splitting rate values coincided with the instant when the upstream demand was reduced (time instant 2500), and this redirected the sections subject to the higher flows from the ramps to operate at near capacity conditions. If downstream of the control area the adoption of variable speed limits was then sufficient to improve traffic conditions, the ill-effect of propagating congestion upstream was contained spatially and temporally by the best use of the remaining network capacity possible through the information provided to users.

To further investigate the traffic behavior in section 55, the evolution of density, ramp queuing and flow values are shown in Figure 12, where simulated values using VSLs and user information are shown in light blue, outputs of the VSL strategy are shown in yellow, and results obtained in the absence of control strategies are shown in red.

The comparison of the density values showed that a clear reduction could only be achieved by reducing the main corridor supply. The steady-state values it was able to achieve were the same as in the other two simulations but occurred much earlier in time. This was also reflected in the detected flows, which were slightly lower than the other simulations because of the different distribution of vehicles within the network. The greatest benefit obtained from this integrated strategy, however, concerned the number of vehicles in the queue, which reached a maximum length of sixteen vehicles (94% less

than what was obtained without the strategy) and remained for considerably less time, following the same initial trend obtained with the use of variable speed limits alone.

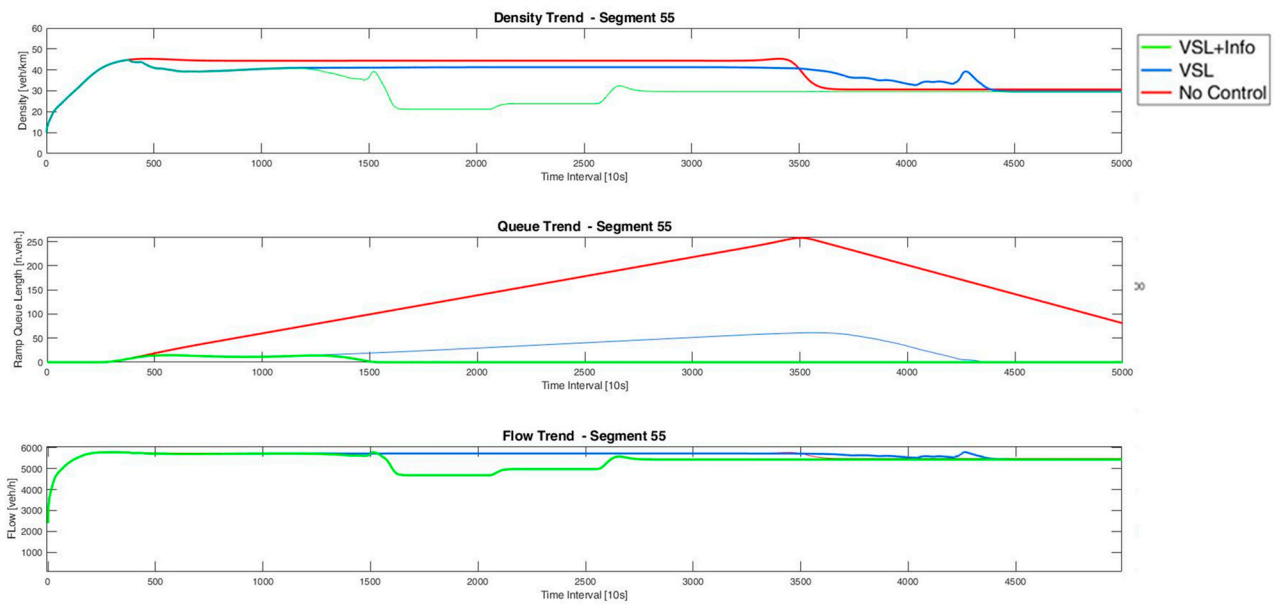


**Figure 12.** Variation over time of density, ramp queue length, and crossing flows in section 55, corresponding to the intersection with State Road 13.

The rapid decrease in density values resulting from the inflows resulted in a higher concentration of detected traffic states around the stable branch of the FD. It occurred earlier in time than in previous simulations and once the initial splitting rates were restored it persisted without any new fluctuations in values (Figure 13).

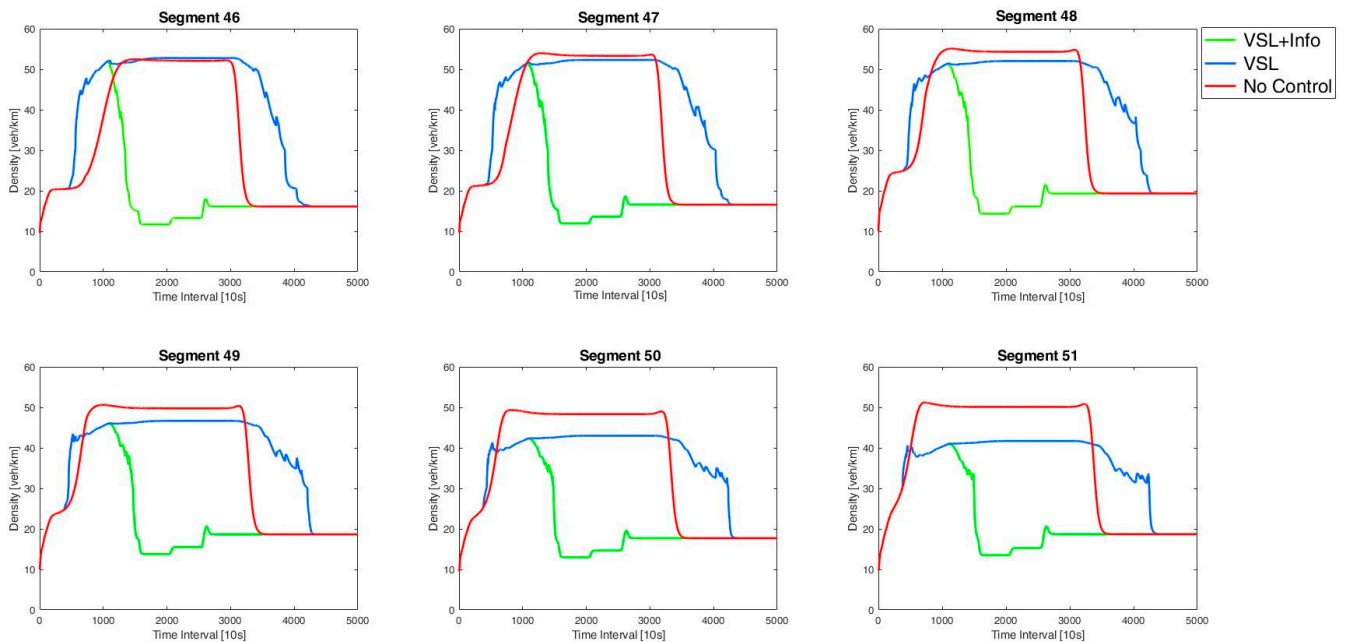


**Figure 13.** Trend of density from segment 46 to segment 51.

Concerning the effects of this strategy on the Mestre Bypass (A4), the impacts on density values were not relevant and the highest values (about 16 veh/km) coincided with the increase in flows coming from upstream. The latter were mainly crossing the corridor and thus remained constant until the intersection with the A27, which was used to merge again with the A57. Vehicles did not continue entirely on the Bypass but divided between it

and the A57, greatly increasing the overall disposal capacity of the network. In case of high flows from the area surrounding Mestre, it was then useful to try to exploit the remaining capacity of the entire network and not of individual corridors. Further confirmation of this was seen by observing the benefits of this intervention at the network level through Total Time Spent (TTS) and Total Travel Distance (TTD).

As expected, the TTS on the Ring Road decreased by 22% compared to a slight increase on the Bypass (Table 2). However, this increase did not directly translate into a delay for vehicles traveling on this infrastructure but was related to the increase in the number of vehicles on the road and the TTD, which was 41% more. At the network level, this integrated strategy allowed for a reduction in TTS of 5.17% and an increase in TTD of 6.25%, in addition to the significant benefits on the on-ramps and safety.

**Table 2.** Comparison of TTS and TTD indicators on major corridors and at the network level among No Control, VSL and VSL integrated with user's information strategies application.

	No Control	VSL	Variation [%]	VSL + Info	Variation [%]
TTS on Ring Road (A57) [veh × h]	33,530	34,740	3.61%	26,130	−22.07%
TTS on Bypass (A4) [veh × h]	53,850	53,850	-	56,730	5.35%
TTS on Network [veh × h]	87,380	88,590	1.38%	82,860	−5.17%
TTD on Ring Road (A57) [veh × km]	2,470,130	2,470,820	0.03%	235,690	−90.46%
TTD on Bypass (A4) [veh × km]	768,040	768,040	-	1,083,660	41.09%
TTD on Network [veh × km]	3,238,170	3,238,870	0.02%	3,440,560	6.25%

Concerning the environment impact, as it is well known in the literature that the speed range with the lowest emissions is between 70 and 90 km/h. Therefore, with the adoption of VSLs and user information, we moved to a speed range that was better from the point of view of emissions.

Summarizing the obtained results, in the first event of the case study, congestion formation was assumed immediately downstream of the area subjected to the control strategy. The use of VSLs reduced the maximum queue length on the on-ramps by 75%, managing to assign the entire vehicular demand that in the absence of control would be locked in the origin section. On the other hand, using the strategy accelerated the propagation of the congestion state on the main corridor and increased its length. Starting from the sections subject to control, the density values were significantly reduced while keeping the crossing flow value unchanged: this condition, therefore, described the transition from the congested section to a stable and safer condition for vehicles.

Nevertheless, the overall time spent on the network was increased because the benefits downstream of the control area were not sufficient to compensate for the negative effects caused upstream. However, the on-ramps were not represented except as centroids: this means that the effects caused by queue propagation on the secondary network were not simulated and thus the benefits induced by improved flow traffic conditions on that network were neglected.

To improve the time spent on the network, the integration of VSLs with user information on the presence of congestion was proposed. In this way, flows were redistributed between the Mestre Bypass and the Ring Road, achieving a 5% reduction in TTS and a 6% increase in TTD, i.e., reducing the overall network time despite the increase in assigned flows.

However, these benefits were due to the case study characteristics, such as mainly the presence of crossing demand and the presence of a high-performance alternative infrastructure.

In the second event studied, the benefits of the strategy were evaluated when the bottleneck was located seven kilometers away from the control sections. In the case of using VSLs, the results showed clear benefits between the control sections and the bottleneck, with stable conditions being achieved and on-ramp flows completely served. Upstream of these sections, there were no significant travel time saving benefits. Integration with user information still did not provide the expected benefits because control strategies were not activated until a congested state was detected in the area subjected to VSLs: the congested

state spread excessively along the infrastructure and the redistribution of demand was almost coincident with the normal reduction in demand because of matrix variation.

## 5. Conclusions

This paper dealt with the study of variable speed limits for traffic control on highways and their integration with user information strategies.

A case study of the Veneto highway network surrounding the locality of Mestre (VE) was presented. The study was carried out using the Dynameq microsimulation software for assigning the demand and the METANET macroscopic model to simulate the progress of the traffic state, reproducing two different cases of road congestion caused by the presence of on-ramps.

From an overall assessment, VSL activators of the MTFC were able to promote ramp flows by anticipating a state of controlled congestion on the mainstream. The network under study consisted of a high density of on-ramps and off-ramps, which did not allow the full benefits of this strategy to be exploited, which need to be optimized by being able to take advantage of a long highway corridor with no intersections. The METANET model as macroscopic was also unable to evaluate vehicle interactions at off-ramps, and thus, there was the possibility of vehicle obstruction because of congestion in the mainstream.

Moreover, an accurate representation of the secondary network and queue propagation on the ramps would allow the benefits of this strategy to be observed, without considering only the primary network.

The results of the application of the two strategies, which were the VSLs and the VSLs integrated with the user information, highlighted the advantages and disadvantages of the different strategies.

Specifically, VSLs prevented queue propagation on the ramp and secondary network blockage. This strategy led to an achievement of greater stability and safety at the same flow or density. The integration with user information optimized the remaining network capacity without penalizing the Bypass.

Disadvantages included the upstream propagation of the kinematic wave being greater and requiring suitable areas to control it. Furthermore, the upstream delays were sometimes greater than the downstream benefits. Finally, an integrated strategy required adequate transportation supply and mainly crossing demand.

Possible developments aimed at deepening the effectiveness of MTFC involve integrating VSLs with other demand control strategies such as ramp metering. Finally, the possibility of varying the control algorithm was suggested. The strategy adopted was activated only upon the detection of a state of congestion within the control sections; therefore, the effect was reactive and it only allowed for the mitigation of negative impacts by reducing speed limits to the minimum value allowed. The use of a proactive approach for determining VSLs would make the best use of the corridor's capacity by preventing the formation of capacity drop phenomena or delaying the propagation of the congestion state over time.

**Author Contributions:** Conceptualization, E.C. and L.M.; methodology, E.C., L.G., and L.M.; software, L.G. and L.M.; validation, E.C., L.G.; formal analysis, E.C. and L.M.; investigation, E.C., L.G. and L.M.; resources, E.C., L.G. and L.M.; data curation, L.G.; writing—original draft preparation, E.C. and L.M.; visualization, L.G. and L.M.; supervision, E.C. and L.M. All authors have read and agreed to the published version of the manuscript.

**Funding:** This research received no external funding.

**Institutional Review Board Statement:** Not applicable.

**Informed Consent Statement:** Not applicable.

**Data Availability Statement:** Not applicable.

**Conflicts of Interest:** The authors declare no conflict of interest.

## References

1. Hegyi, A.; DeSchutter, B.; Hellendoorn, J. Optimal Coordination of Variable Speed Limits to Suppress Shock Waves. *IEEE Trans. Intell. Transp. Syst.* **2005**, *6*, 102–112. [[CrossRef](#)]
2. Chen, J.; Yu, Y.; Guo, Q. Freeway Traffic Congestion Reduction and Environment Regulation via Model Predictive Control. *Algorithms* **2019**, *12*, 220. [[CrossRef](#)]
3. Kotsialos, A.; Papageorgiou, M.; Diakaki, C.; Pavlis, Y.; Middelham, F. Traffic flow modeling of large-scale motorway networks using the macroscopic modeling tool METANET. *IEEE Trans. Intell. Transp. Syst.* **2002**, *3*, 282–292. [[CrossRef](#)]
4. Smulders, S. *Control by Variable Speed Signs—The Dutch Experiment*; Ministry of Transport: Amsterdam, The Netherlands, 1992.
5. Smulders, S.; van den Hoogen, E. Control by variable speed signs: Results of the Dutch experiment. In Proceedings of the Seventh International Conference on Road Traffic Monitoring and Control, London, UK, 26–28 April 1994; pp. 145–149.
6. Bertini, R.L.; Boice, S.; Bogenberger, K. Dynamics of Variable Speed Limit System Surrounding Bottleneck on German Autobahn. *Transp. Res. Rec.* **2006**, *1978*, 149–159. [[CrossRef](#)]
7. Chung, W.; Abdel-Aty, M.; Park, H.-C.; Cai, Q.; Rahman, M.; Gong, Y.; Ponnaluri, R. Development of Decision Support System for Integrated Active Traffic Management Systems Considering Travel Time Reliability. *Transp. Res. Rec. J. Transp. Res. Board* **2020**, *2674*, 167–180. [[CrossRef](#)]
8. Dong, C.; Shao, C.; Richards, S.H.; Han, L.D. Flow rate and time mean speed predictions for the urban freeway network using state space models. *Transp. Res. Part C Emerg. Technol.* **2014**, *43*, 20–32. [[CrossRef](#)]
9. Varotto, S.F.; Jansen, R.; Bijleveld, F.; van Nes, N. Driver speed compliance following automatic incident detection: Insights from a naturalistic driving study. *Accid. Anal. Prev.* **2020**, *150*, 105939. [[CrossRef](#)] [[PubMed](#)]
10. Cipriani, E.; Gori, S.; Mannini, L. Traffic state estimation based on data fusion techniques. In Proceedings of the 15th International IEEE Conference on Intelligent Transportation Systems, Anchorage, AK, USA, 16–19 September 2012; pp. 1477–1482.
11. Cipriani, E.; Gori, S.; Mannini, L.; Brinchi, S. A procedure for urban route travel time forecast based on advanced traffic data: Case study of Rome. In Proceedings of the 17th International IEEE Conference on Intelligent Transportation Systems (ITSC), Qingdao, China, 8–11 October 2014; pp. 936–941. [[CrossRef](#)]
12. Marzano, V.; Papola, A.; Simonelli, F.; Papageorgiou, M. Fellow A Kalman Filter for Quasi-Dynamic o-d Flow Estimation/Updating. *IEEE Trans. Intell. Transp. Syst.* **2018**, *19*, 3604–3612. [[CrossRef](#)]
13. Roy, K.C.; Hasan, S.; Culotta, A.; Eluru, N. Predicting traffic demand during hurricane evacuation using Real-time from transportation systems and social media. *Transp. Res. Part C* **2021**, *131*, 103339. [[CrossRef](#)]
14. Cremer, M. *Der Verkehrsfluß auf Schnellstrassen*; Springer: Berlin/Heidelberg, Germany, 1979.
15. Zackor, H. Speed Limitation on Freeways: Traffic-Responsive Strategies. In *Concise Encyclopedia of Traffic and Transportation Systems*; Papageorgiou, M., Ed.; Pergamon Press: Oxford, UK, 1991; pp. 507–511.
16. Papageorgiou, M.; Kosmatopoulos, E.; Papamichail, I. Effects of Variable Speed Limits on Motorway Traffic Flow. *Transp. Res. Rec. J. Transp. Res. Board* **2008**, *2047*, 37–48. [[CrossRef](#)]
17. Wang, Y.; Papageorgiou, M.; Messmer, A. Real-time freeway traffic state estimation based on extended Kalman filter: Adaptive capabilities and real data testing. *Transp. Res. Part A Policy Pract.* **2008**, *42*, 1340–1358. [[CrossRef](#)]
18. Alasiri, F.; Zhang, Y.; Ioannou, P.A. Robust variable speed limit control with respect to uncertainties. *Eur. J. Control.* **2021**, *59*, 216–226. [[CrossRef](#)]
19. Bie, Y.; Seraj, M.; Zhang, C.; Qiu, T.Z. Improving Traffic State Prediction Model for Variable Speed Limit Control by Introducing Stochastic Supply and Demand. *J. Adv. Transp.* **2018**, *2018*, 7959815. [[CrossRef](#)]
20. Yu, R.; Abdel-Aty, M. An optimal variable speed limits system to ameliorate traffic safety risk. *Transp. Res. Part C Emerg. Technol.* **2014**, *46*, 235–246. [[CrossRef](#)]
21. Wang, X.; Zhang, R.; Gou, Y.; Liu, J.; Zhao, L.; Li, Y. Variable Speed Limit Control Method of Freeway Mainline in Intelligent Connected Environment. *J. Adv. Transp.* **2021**, *2021*, 8863487. [[CrossRef](#)]
22. Gao, H.; Cheng, S.; Zhang, M. *Get More out of Variable Speed Limit (VSL) Control: An Integrated Approach to Manage Traffic Corridors with Multiple Bottleneck*; Research Report from the Pacific Southwest Region University Transportation Center 2020; UC Davis Institute of Transportation Studies: Davis, CA, USA, 2020.
23. Carlson, R.C.; Papamichail, I.; Papageorgiou, M.; Messmer, A. Optimal mainstream traffic flow control of large-scale motorway networks. *Transp. Res. Part C Emerg. Technol.* **2009**, *18*, 193–212. [[CrossRef](#)]
24. Lu, Q.; Tettamanti, T. Impacts of autonomous vehicles on the urban fundamental diagram. In Proceedings of the 5th International Conference on Road and Rail Infrastructure, CETRA 2018, Zadar, Croatia, 17–19 May 2018.
25. Olia, A.; Razavi, S.; Abdulhai, B.; AbdelGawad, H. Traffic capacity implications of automated vehicles mixed with regular vehicles. *J. Intell. Transp. Syst.* **2018**, *22*, 244–262. [[CrossRef](#)]
26. Gemma, A.; Cipriani, E.; Crisalli, U.; Mannini, L. Automated Vehicles' Effects on Urban Traffic Flow Parameters. In *Smart Energy for Smart Transport. CSUM 2022; Lecture Notes in Intelligent Transportation and Infrastructure*; Nathanail, E.G., Gavanis, N., Adamos, G., Eds.; Springer: Cham, Switzerland, 2023.
27. Vrbanić, F.; Ivanjko, E.; Kušić, K.; Čakija, D. Variable Speed Limit and Ramp Metering for Mixed Traffic Flows: A Review and Open Questions. *Appl. Sci.* **2021**, *11*, 2574. [[CrossRef](#)]
28. Xia, X.; Meng, Z.; Han, X.; Li, H.; Tsukiji, T.; Xu, R.; Zhang, Z.; Ma, J. Automated Driving Systems Data Acquisition and Processing Platform. *arXiv* **2022**, arXiv:2211.13425.

29. Gao, L.; Xiong, L.; Xia, X.; Lu, Y.; Yu, Z.; Khajepour, A. Improved Vehicle Localization Using On-Board Sensors and Vehicle Lateral Velocity. *IEEE Sens. J.* **2022**, *22*, 6818–6831. [[CrossRef](#)]
30. Khondaker, B.; Kattan, L. Variable speed limit: A microscopic analysis in a connected vehicle environment. *Transp. Res. Part C Emerg. Technol.* **2015**, *58*, 146–159. [[CrossRef](#)]
31. Hadiuzzaman, M.; Qiu, T.Z. Cell transmission model based variable speed limit control for freeway. In Proceedings of the 91st Transportation Research Board Annual Meeting, Washington, DC, USA, 22–26 January 2012.
32. Yuan, T.; Alasiri, F.; Zhang, Y.; Ioannou, P.A. Evaluation of Integrated Variable Speed Limit and Lane Change Control for Highway Traffic Flow. *IFAC-Pap.* **2021**, *54*, 107–113. [[CrossRef](#)]
33. Raadsen, M.P.; Bliemer, M.C. Variable speed limits in the link transmission model using an information propagation method. *Transp. Res. Part C Emerg. Technol.* **2021**, *129*, 103184. [[CrossRef](#)]
34. Khondaker, B.; Kattan, L. Variable speed limit: An overview. *Transp. Lett.* **2015**, *7*, 264–278. [[CrossRef](#)]
35. Messner, A.; Papageorgiou, M. METANET: A macroscopic simulation program for motorway networks. *Traffic Eng. Control* **1990**, *31*, 466–470.
36. Mazaré, P.-E.; Dehwah, A.H.; Claudel, C.G.; Bayen, A.M. Analytical and grid-free solutions to the Lighthill–Whitham–Richards traffic flow model. *Transp. Res. Part B Methodol.* **2010**, *45*, 1727–1748. [[CrossRef](#)]
37. Wang, Y.; Papageorgiou, M. Real-time freeway traffic state estimation based on extended Kalman filter: A general approach. *Transp. Res. Part B* **2005**, *39*, 141–167. [[CrossRef](#)]

**Disclaimer/Publisher’s Note:** The statements, opinions and data contained in all publications are solely those of the individual author(s) and contributor(s) and not of MDPI and/or the editor(s). MDPI and/or the editor(s) disclaim responsibility for any injury to people or property resulting from any ideas, methods, instructions or products referred to in the content.